Journal of the European Ceramic Society **13** (1994) 371–378

Nanometric Boron Nitride Powders: Laser Synthesis, Characterization and FT-IR Surface Study

M. I. Baraton,[a] L. Boulanger,[b] M. Cauchetier,[c] V. Lorenzelli,[d] M. Luce,[c] T. Merle,[a] P. Quintard[a] & Y. H. Zhou[c]

[a] Laboratoire de Matériaux Céramiques et Traitements de Surface, URA 320 CNRS, 123 Ave Albert Thomas, F-87060 Limoges, France
[b] CEA-CEREM-DTM-SRMP-CE, Saclay, F-91191 Gif-sur-Yvette, France
[c] CEA-DSM-DRECAM-SPAM-CE, Saclay, F-91191 Gif-sur-Yvette, France
[d] Istituto di Chimica, Facoltà di Ingeneria, Ple Kennedy, I-16129 Genova, Italy

(Received 5 July 1993; revised version received 3 November 1993; accepted 10 November 1993)

Abstract

Boron nitride powders in the nanometric range were synthesized by laser driven reactions in BCl_3–NH_3 mixtures. The gaseous reactants were separately introduced in the beam of a high-powered continuous wave CO_2 laser. The powders with high specific surface area (up to 230 $m^2 g^{-1}$) present the turbostratic structure as characterized by TEM. The evolution towards the hexagonal structure by heating the powders up to 1920 K under nitrogen flow was followed by XRD. One BN powder has been fully characterized by infrared and Raman spectroscopies regarding bulk structure and identification of surface species as well.

Bornitrid (BN) Pulver mit Nanometer-Korngrößen werden mit Hilfe eines CO_2 Dauerstrichlaser durch Pyrolyse aus dem Gasgemisch BCl_3–NH_3 gewonnen. Die Pulver mit hochspezifischer Oberfläche (bis zu 230 $m^2 g^{-1}$) weisen eine 'turbostratische' Struktur auf, wie eine TEM-Analyse es gezeigt hat. Die Entwicklung hin zur hexagonalen Struktur durch Erwärmung des Pulvers auf 1920 K unter Stickstoff wird von XRD gefolgt. Eines der BN Pulver konnte durch Infrarot- und Ramanspektroskopie vollständig charakterisiert werden, wobei außerdem chimisorbierte 'Oberflächengruppen' identifiziert wurden.

Par pyrolyse de mélanges gazeux de BCl_3 et de NH_3, introduits séparément dans le faisceau d'un laser CO_2 continu, on synthétise des poudres nanométriques de nitrure de bore. La surface spécifique des poudres peut atteindre 230 $m^2 g^{-1}$. Une analyse MET met en évidence une structure turbostratique. L'évolution vers la structure hexagonale par chauffage des poudres sous flux d'azote jusqu'à 1920 K est suivi par DRX. On a caractérisé complètement une poudre de BN par spectrométrie infrarouge (FT-IR) et Raman, de plus les groupements chimisorbés en surface ont été identifiés.

1 Introduction

An attractive and innovative method for the preparation of ultrafine powders was initiated by Flint & Haggerty.[1] Gaseous or volatile precursors were pyrolyzed with a CO_2 laser. This process was mainly used for the synthesis of nanoscale Si-based powders: Si, SiC, Si_3N_4, Si/C/N composites[1,2] using gaseous precursors. Recently liquid Si-based precursors have been injected into the laser beam as fine droplets of an aerosol.[3,4] Boron-containing powders were also synthesized: B and TiB_2,[5] B_4C[6] and BN.[7] In this paper are presented some results concerning the laser synthesis of boron nitride from BCl_3–NH_3 mixtures and its full characterization by infrared (FT-IR) and Raman spectroscopies regarding bulk structure and identification of surface species as well.

2 Experimental

The experimental device is pictured in Fig. 1 and has already been described.[7] The two reagents—BCl_3 and NH_3—have absorption bands near the emission line of the CO_2 laser in the 10·6 μm range. The

Journal of the European Ceramic Society 0955-2219/94/$7.00 © 1994 Elsevier Science Limited, England. Printed in Great Britain

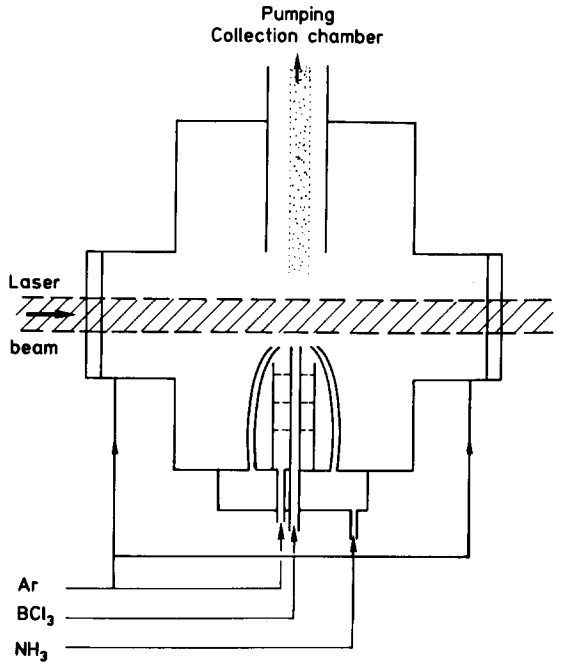

Fig. 1. Schematic of the irradiation cell (total length = 280 mm).

reagents are introduced separately in the laser beam because they react at room temperature to give a white solid adduct. The nozzle systems with different gas outlet geometries are shown in Fig. 2. Best results are obtained with nozzles 2b and 2d.

The powders were analyzed and characterized by X-ray diffraction (XRD), transmission electronic microscopy (TEM) and electron diffraction in the TEM; particle size was calculated from BET surface area determination. The O_2 content was obtained from energy dispersive spectroscopy (EDS) in TEM equipped with a low element detector and using a ratio technique with SiO_2 and Si_3N_4 standards.[8]

The infrared spectra were recorded on a Nicolet 5DX spectrometer using two sampling methods. Firstly, the bulk spectrum was obtained from standard KBr pellets (concentration 0·2–0·5 wt%). Secondly, as the surface investigation required a large amount of powder, pure boron nitride was pressed into grid-supported pellets (Inox grid from Gantois, Saint-Dié, France) for better handling and heat spreading. In either method, the recording range is from 4000 to 400 cm^{-1} with a 4 cm^{-1} resolution.

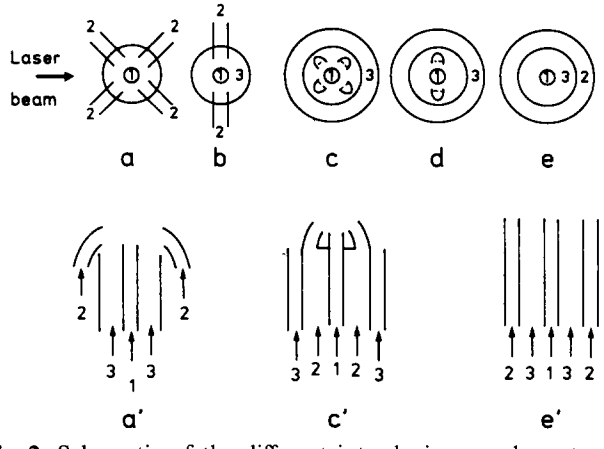

Fig. 2. Schematic of the different introducing nozzle systems

A vacuum line allows thermal treatment (up to 870 K) of the samples in order to obtain better evidence of the surface species and of their reactivity under different pressures of controlled atmosphere. All experiments are run *in situ*, inside the sample chamber of the spectrometer.

The Raman scattering measurements were carried out on a Dilor microprobe with a double monochromator and using the 514·5 nm Ar ion laser radiation. Under the microscope, each analyzed spot gives the same spectrum, proving the powder to be homogeneous on this scale.

D_2 (from Alphagaz, 99·99% pure) underwent no further purification and methanol (from Prolabo, Normapur) was dried on molecular sieves prior to use.

The change in the structure (turbostratic → hexagonal) was followed by XRD after thermogravimetric analysis (TGA) under flowing N_2 between 1270 K and 1920 K using the model STA409 from Netzsch, Selb, Germany.

3 Synthesis and Bulk Characterization

3.1 Laser synthesis

The experimental conditions and the connected results are summarized in Table 1. The overall reaction is:

$$BCl_3 + NH_3 \rightarrow BN + 3HCl$$

and an excess of NH_3 reacts with HCl to give NH_4Cl as by-product. NH_4Cl formed in the hot zone as gas phase diffuses through the cell and condenses into solid form on the cold walls of the reactor. No indication of a flame temperature (> 1220 K) from hot particles as Refs 1–5 is given by the optical pyrometer, even if a high white luminous zone is formed at the intersection of the laser beam with the reactant gases. The plunging tubing which leads to

Table 1. Results on BN powder synthesis, according to experimental parameters: flow rate, laser power and irradiation nozzle geometry

Run	*Flow rates* (cm^3/min)		*Laser power* (W)	*Irradiation geometry*	*Yield* (g/h)	S_{BET} (m^2/g)
	NH_3	BCl_3				
2	500	100	600	a	38·8	—
3	500	100	400	b	40	185
13	180	80	600	d	7·4	85
16	400	100	400	d	23	234
17	400	100	400	d	23	141

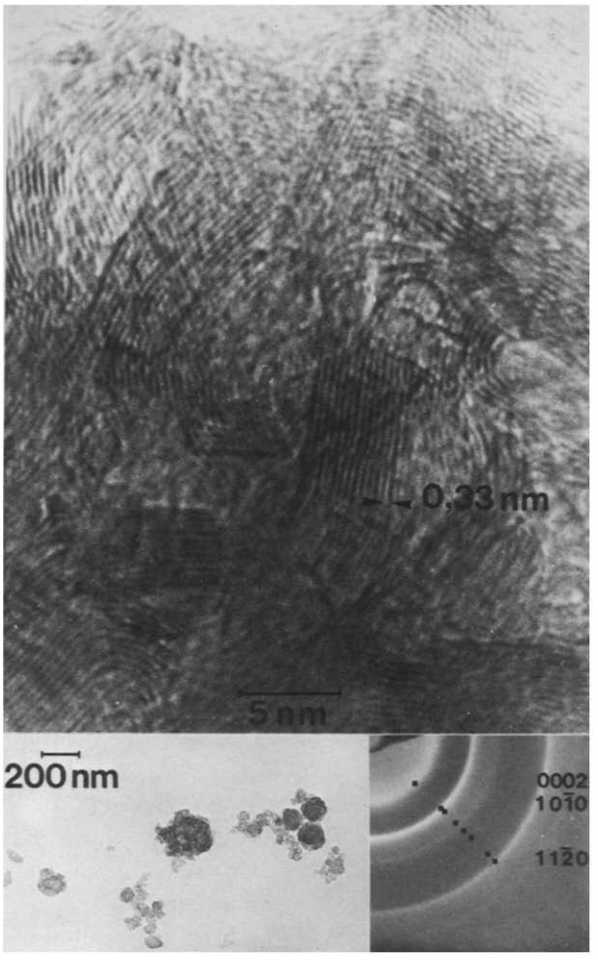

Fig. 3. TEM photograph of BN particles with corresponding electron diffraction pattern.

the collection chamber is obstructed by the deposition of $BN–NH_4Cl$ mixtures. Improvements are expected by heating all the collection device at a temperature greater than the sublimation temperature of NH_4Cl, namely 631 K. NH_4Cl is eliminated from the solid mixture by water washing or by heating under flowing nitrogen at 770–870 K.

The particle size calculated from BET measurements varies from 11 to 31 nm.

The oxygen content determined by EDS is 7 ± 2 wt% in a powder which has been water-washed then dried at 350 K. Equivalent values were obtained for other BN powders prepared from pyrolysis of $BCl_3–NH_3$ mixtures.[9] The effect of the surface area on the oxygen content did not appear significant within the experimental conditions reported here.

3.2 TEM analysis

On the low magnification image obtained by TEM as shown in Fig. 3 it appears that grain filaments wound in balls form fine particles which are characteristic of the graphite-like turbostratic structure. The high-resolution image shows the atomic planes separated by a 0·35 nm distance. The corresponding electron diffraction pattern has only three rings of the hexagonal lattice: 002, 100 and 110, five rings being missing.

The turbostratic structure is derived from graphite: the stacking of flat B_3N_3 hexagons, still nearly parallel, is no longer regular with respect to the alternate alignment of the atoms in the different planes.[10,11] Nevertheless, the short-range order is the same as in the hexagonal crystallization.

3.3 Raman and FT-IR characterization

Characterizations by Raman and IR spectroscopies have been focused on sample 17 of Table 1. Crystallized hexagonal BN (h-BN) has $D6h/4$ space group symmetry and the irreducible representation for the normal modes is:[12,13]

$$\Gamma = 2E_{2g}(\mathrm{R}) + 2B_{1g}(\mathrm{inact.}) + A_{2u}(\mathrm{IR}) + E_{1u}(\mathrm{IR})$$

The two Raman modes in a highly oriented crystal are observed at 1366·2 and 51·2 cm^{-1}. Whereas the high-wavenumber band corresponds to B and N

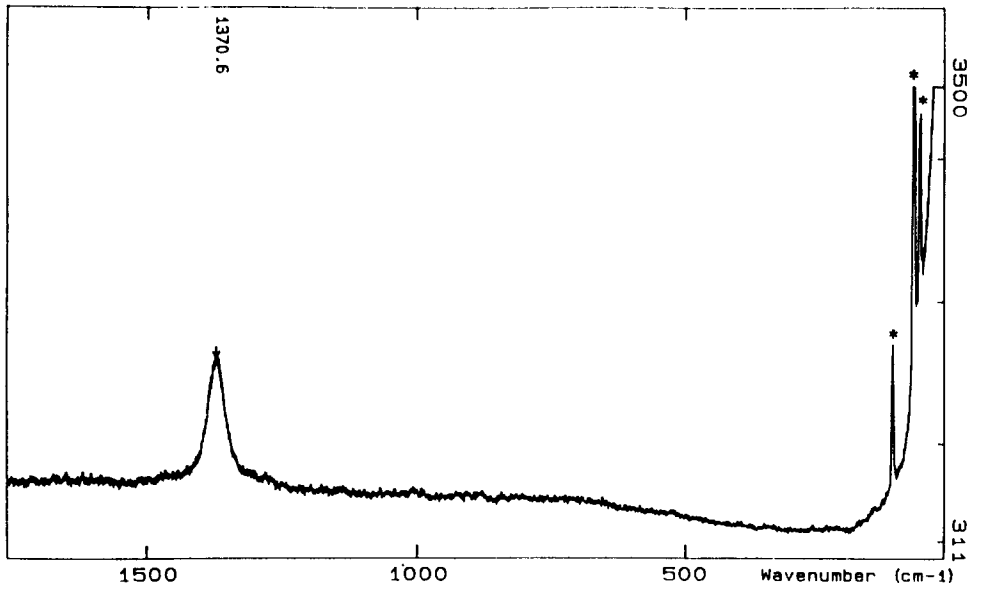

Fig. 4. Micro-Raman spectrum of boron nitride (* plasma lines).

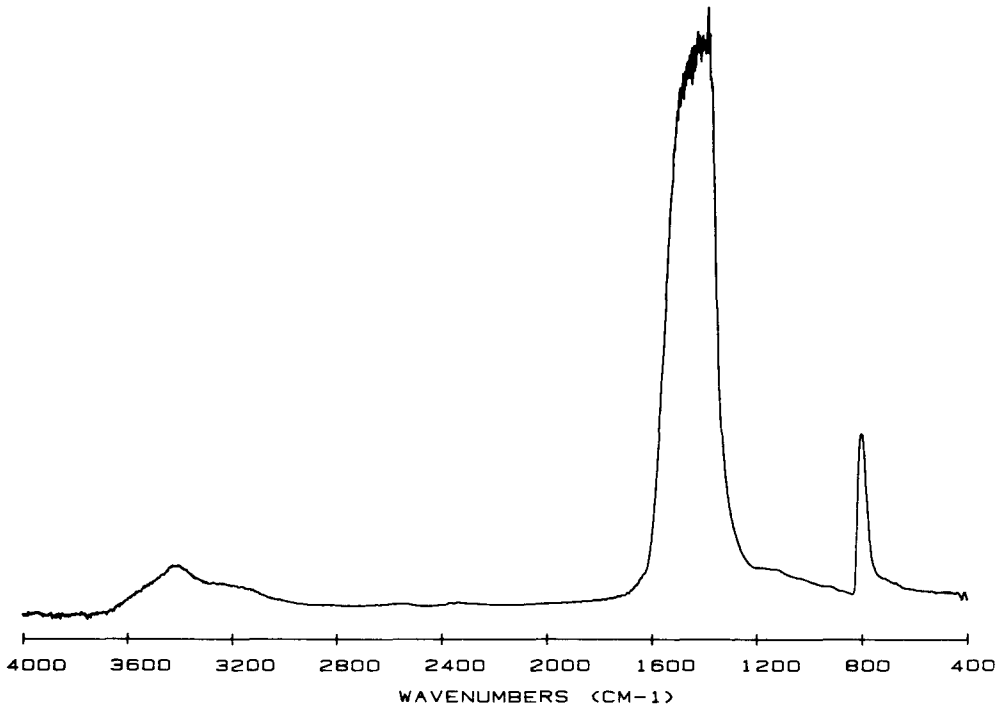

Fig. 5. Infrared spectrum of BN powder (in KBr pellet, concentration 0·2 wt%).

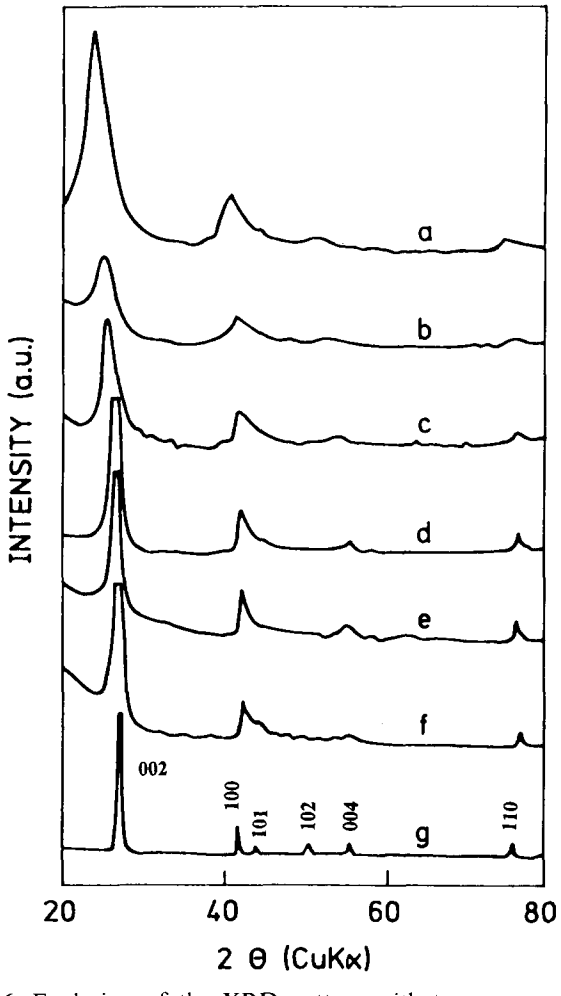

Fig. 6. Evolution of the XRD pattern with temperature: a, 350 K (after washing); b, 1270 K; c, 1470 K; d, 1670 K; e, 1870 K; f, 1920 K; g, commercial powder.

atoms moving against each other in a plane, the low-wavenumber frequency is due to the whole planes sliding against each other, the reason for such a difference being the large anisotropy of inter- and intraplaning bonds.[12] This latter frequency no longer exists in microcrystalline powders. The Raman spectrum of the present sample (Fig. 4) presents the high wavenumber band (1372 cm^{-1}), notably broader than in well-crystallized boron nitride as a result of the decrease of the ordered domains.

As for the infrared spectrum (Fig. 5), both absorption frequencies (1410 and 809 cm^{-1}) are close to the ones of h-BN (1373 and 816 cm^{-1}),[14] by virtue of the similar short-range order which is infrared sensitive. The higher-wavenumber absorption is assigned to the stretching mode and the lower one to the deformation mode.[15] The broad band centered at ~3500 cm^{-1} is due to adsorbed surface species and will be discussed later.

3.4 Evolution of the structure by annealing

The change in the structure after heating treatment is followed by X-ray diffraction as shown in Fig. 6. Below 1470 K only three diffused reflections are present, i.e. 002, 100 and 110. The degree of the ordering in the crystal lattice increases with heating temperature and the value of the interplanar spacing in the (002) direction remains greater than the standard value of a commercial coarse powder (Fig. 7). As explained in Ref. 16 the transition from the turbostratic structure (two-dimensional) to the well-ordered hexagonal structure (three-dimensional) is not related to a microdiffusion phenomenon.

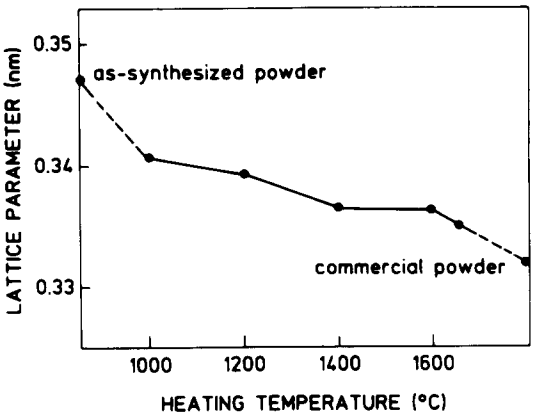

Fig. 7. Evolution of d_{002}, interplanar spacing in the (002) direction.

4 Surface species analysis

The infrared spectrum of a grid-supported pellet does not offer large transparency windows. Below 1600 cm^{-1} the absorption is due to the skeletal vibrations whose 2330 and 2550 cm^{-1} absorption frequencies are the associated overtones and/or combination bands.[15] These last two bands can hardly be seen in the bulk spectrum (Fig. 5).

A step-by-step activation consists in heating the sample under vacuum (usually 5×10^{-6} mbar). Then at each temperature chosen as a stage, the sample is cooled down to room temperature still under vacuum prior to recording the spectrum. This procedure allows the evolution of the absorption bands to be followed. The tremendous difference (Fig. 8) in the high-wavenumber region corresponds to the departure of the physisorbed or weakly chemisorbed species, i.e. mainly water due to the atmospheric contamination. Physisorbed water is completely eliminated at 470 K, clearing the 3000 cm^{-1} region. Concomitantly three bands begin to stand out. The subsequent activation up to 770 K achieves their profile steadily and the three absorption maximums can finally be noted at 3658, 3566 and 3432 cm^{-1}.

The next step in the characterization of the surface species is deuteration. Indeed, all the hydrogen-containing groups accessible to deuterium will see their stretching absorption frequencies shifted downwards in the ratio of 1·36 (in the harmonic oscillator approximation). Deuterium added to the present sample at 770 K (160 mbar for 2 h and 310 mbar for 3 h) removes the above-mentioned three bands, although the 3432 cm^{-1} frequency does not vanish completely (Fig. 9). Three similar bands appear at lower wavenumbers (2700, 2636 and 2545 cm^{-1}) in the 1·35 ratio. The obvious conclusion is that these bands belong to surface species whose stretching vibrations involve hydrogen atoms.

The comparison with vibration frequencies in boron nitride deposits on one hand[17] and of surface groups in mixed oxides on the other hand[18,19] as well as previous findings on a different boron nitride[20] make quite clear the assignments:

—3658 cm^{-1} to ν(OH) stretching vibration in B–OH surface groups (ν(OD) at 2700 cm^{-1});
—3566 and 3432 cm^{-1} to asymmetric and symmetric modes in B–NH_2 surface groups ($\nu(ND_2)$ at 2636 and 2545 cm^{-1}).

These results show the hydrolysis of the surface. However, imido groups B_2–NH are not present on the surface, unlike on another boron nitride from a different preparation process.[20] In this case this lack may be due to the excess of NH_3 during the reaction.

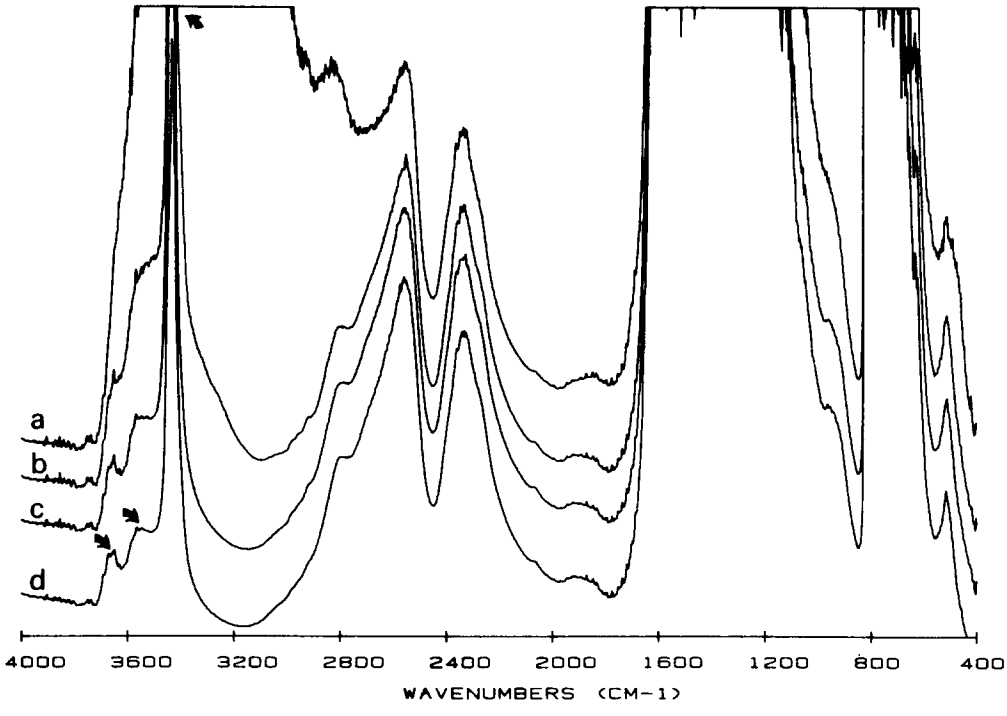

Fig. 8. Step-by-step activation (see text). Infrared spectra at different temperatures: a, room temperature; b, 470 K; c, 670 K; d, 770 K.

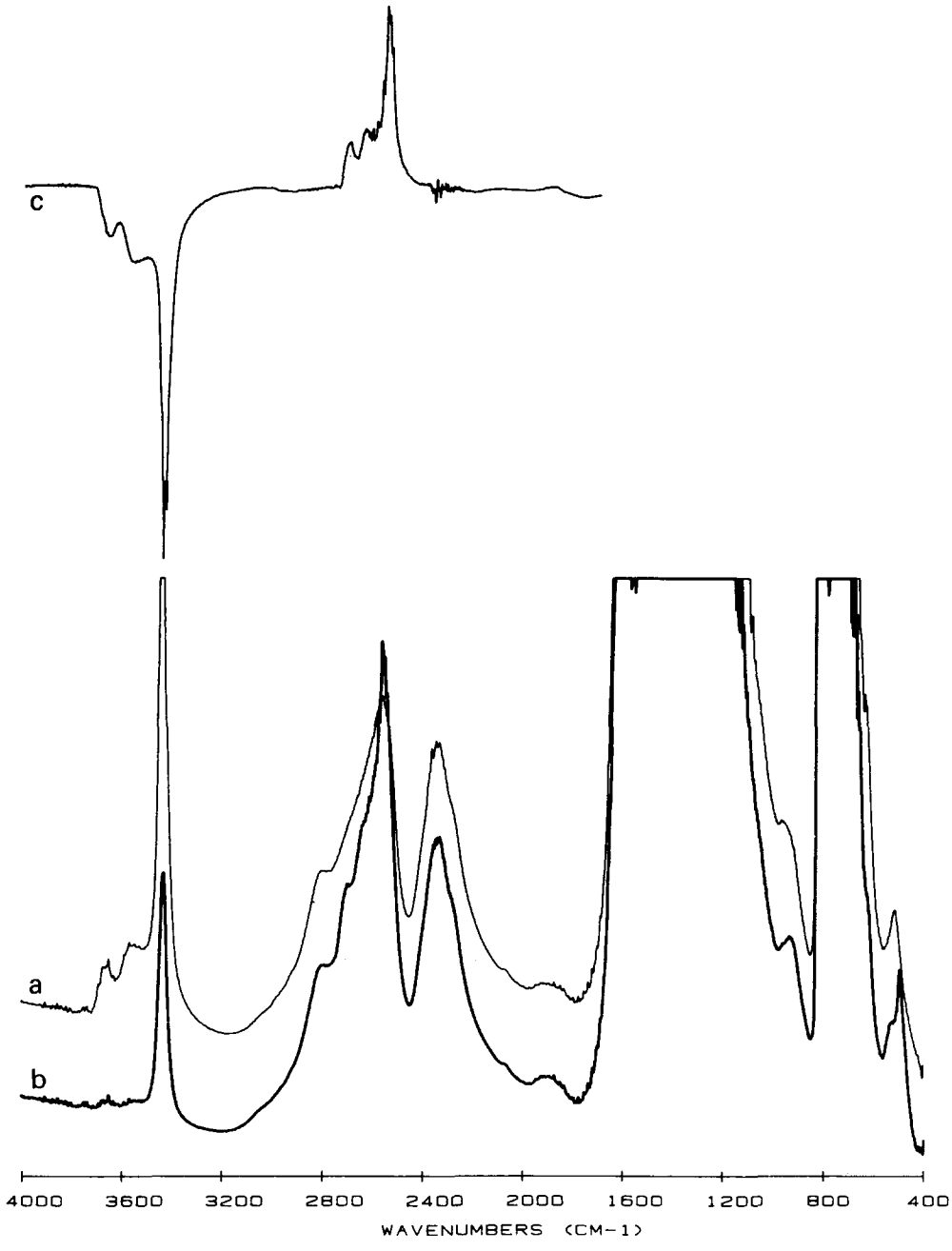

Fig. 9. Deuteration of activated boron nitride. Infrared spectra: a, pure activated sample; b, deuterated sample; c, difference spectrum (b – a). The negative bands correspond to disappearing species and the positive bands to appearing species.

As already noticed in several cases, the OH surface groups are easily deuterated, whereas under the same conditions, the isotopic exchange does not complete in the NH_2 groups.[21-23]

The action of methanol molecules characterizes the lability of the OH surface bonds. 5 mbar of CH_3OH are added to the sample at room temperature for 45 min (Fig. 10(a) and (b)). A subsequent evacuation removes the gaseous species and the weakly hydrogen-bonded methanol. The difference spectrum (Fig. 10(c)) clearly displays the changes occurring on the BN surface: a couple of bands appears at 2960 and 2880 cm^{-1} with a strong broad band centered at ~3550 cm^{-1} while ν(OH) at 3690 cm^{-1} decreases. These bands, created as soon as methanol is added, are assigned to ν(CH) stretching vibrations in the CH_3 groups,[24] whereas the broad ~3550 cm^{-1} band corresponds to the ν(OH) vibration frequency of the surface bonds involved in a hydrogen bond with methanol. Heating up to 770 K under vacuum causes a gentle but incomplete decrease of the ν(CH) bands along with the elimination of the 3500 cm^{-1} band and a partial recovering of the ν(OH) and $\nu(NH_2)$. The reverse behavior of both ν(CH) bands on one hand and of the ν(OH) band on the other hand as well as the thermal stability of the new-formed species prove the methoxylation of the surface:[25,26]

$$B—OH + CH_3OH \rightarrow B—OCH_3 + H_2O$$

A closer look to the spectra shows that the positive and negative bands appearing in the $\nu(NH_2)$ region on the difference spectrum are nothing else but a frequency shift and/or a broadening of the two $\nu(NH_2)$ bands, possibly due to an environmental

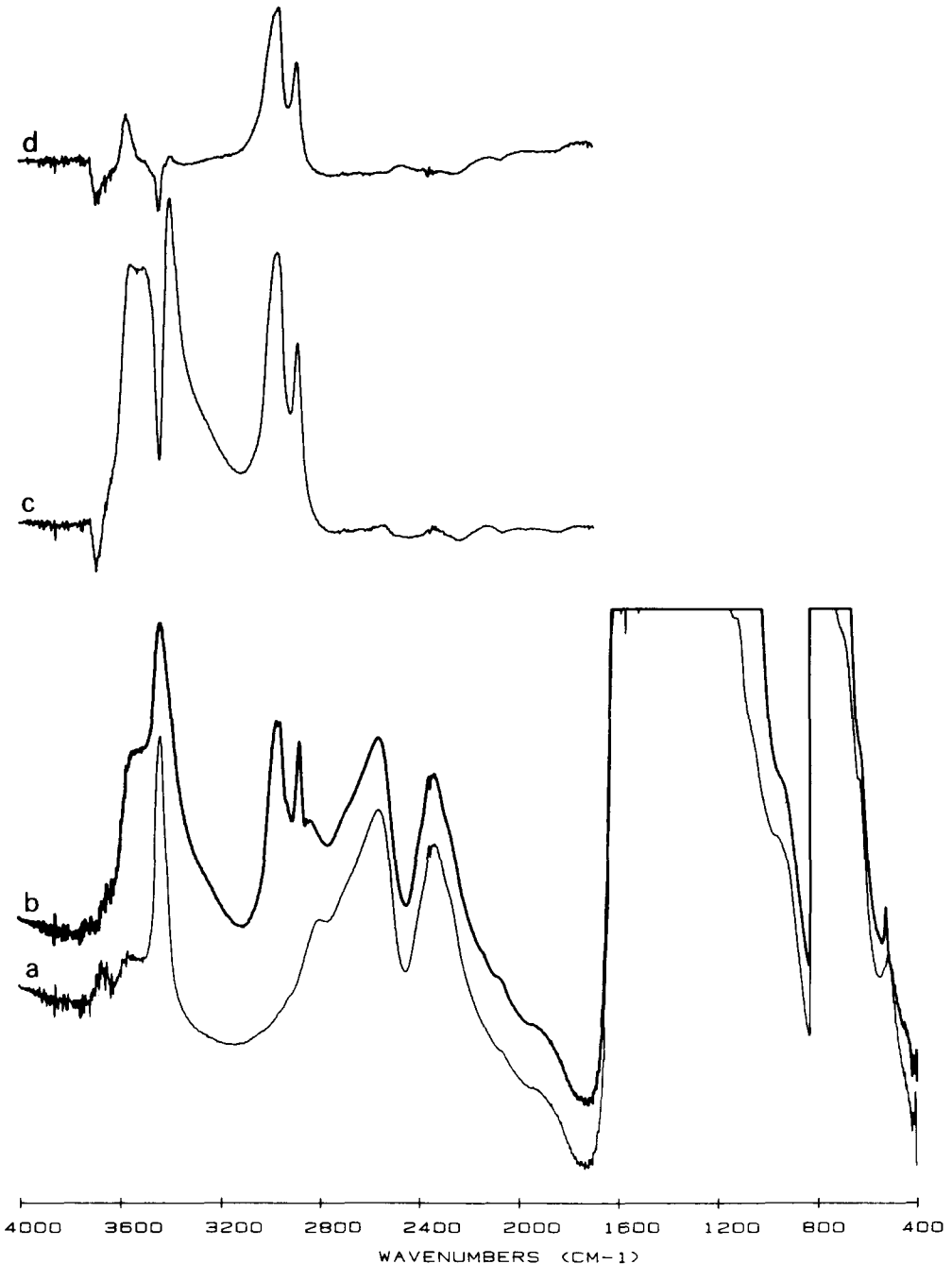

Fig. 10. Methoxylation of BN. Infrared spectra: a, pure activated sample; b, after adding CH_3OH (5 mbar, 45 min); c, after pumping out at room temperature for 30 min (difference spectrum); d, after pumping out at 770 K for 60 min (difference spectrum).

modification, the neighboring groups changing from OH to OCH_3.[15]

5 Conclusion

The pyrolysis process in a CO_2 laser beam can supply ultrafine boron nitride powder. The turbostratic structure is characterized by TEM, infrared and Raman analysis all together. The species present on the surface show the hydrolysis but excess NH_3 in the preparation procedure prevents imido groups B_2–NH from forming. It is worth mentioning that, according to the synthesis process, boron nitride powder may have different surface states even though the bulk structures are very similar. Therefore, it must be kept in mind that any application involving surface species does imply a careful choice of the material's formation process.

References

1. Flint, J. H. & Haggerty, J. S., Models for synthesis of ceramic powders by vapor phase reactions. In *Ceram. Trans., Vol. 1: Ceramic Powder Science II*, ed. G. L. Messing, E. R. Fuller Jr. & H. Hausner. The American Ceramic Society, Westerville, OH, 1988, pp. 244–52.
2. Cauchetier, M., Croix, O., Luce, M., Baraton, M. I., Merle, T. & Quintard, P., Nanometric Si/C/N composite powders: laser synthesis and IR characterization. *J. Eur. Ceram. Soc.*, **8** (1991) 215–19.
3. Gonsalves, K. E., Strutt, P. R., Xiao, T. D. & Clemens, P. G., Synthesis of Si(C,N) nanoparticles by rapid laser polycondensation/crosslinking reactions of an organosilazane precursor. *J. Mater. Sci.*, **27** (1992) 3231–8.
4. Herlin, N., Luce, M., Musset, E. & Cauchetier, M.,

Production of nanocomposite Si/C/N pre-ceramic powders by laser pyrolysis of hexamethyldisilazane. In *Proceedings of the 3rd ECerS Conference*, Vol. 1, 1993, pp. 33–8.
5. Casey, J. D. & Haggerty, J. S., Laser-induced vapor-phase syntheses of boron and titanium diboride powders. *J. Mater. Sci.*, **22** (1987) 737–44.
6. Knudsen, A. K., Laser driven synthesis and densification of ultrafine boron carbide powders. In *Advances in Ceramics, Vol. 21: Ceramic Powder Science*, ed. G. L. Messing, K. S. Mazdiyasni, J. W. McCauley & R. A. Haber. The American Ceramic Society, Westerville, OH, 1987, pp. 237–47.
7. Luce, M., Croix, O., Zhou, Y. H., Cauchetier, M., Sapin, M. & Boulanger, L., Laser synthesis and characterization of ultrafine boron nitride powders. In *Proceedings of the 2nd ECerS Conference*, Vol. 1, 1993, pp. 233–8.
8. Boulanger, L., Unpublished results.
9. Iltis, A. & Magnier, C., Amorphous or turbostratic boron nitride, especially with a spherical morphology and its manufacture. European Patent Application EP-396448, 7 November 1990.
10. Rother, B. & Weissmantel, C., Structure and chemical composition of RF-sputtered boron nitride films. *Phys. Stat. Sol.*, **A87** (1987) K119–21.
11. Rother, B., Zschiele, H. D., Weissmantel, C. *et al.*, Preparation and characterization of ion-plated boron nitride. *Thin Solid Films*, **142** (1986) 83–9.
12. Nemanich, R. J., Solin, S. A. & Martin, R. M., Light scattering study of boron nitride microcrystals. *Phys. Rev. B*, **23** (1981) 6348–56.
13. Geick, R., Perry, C. H. & Rupprecht, G., Normal modes in hexagonal boron nitride. *Phys. Rev.*, **146** (1966) 543–7.
14. Baraton, M. I., Merle, T., Quintard, P. & Lorenzelli, V., FT-IR investigation of surface species on a submicronic boron nitride powder. In *Proceedings of the 2nd ECerS Conference*, Vol. 1, 1993, pp. 251–5.
15. Baraton, M. I., Merle, T., Quintard, P. & Lorenzelli, V., Surface species on a submicronic boron nitride powder. A starting FT-IR characterization. *J. Mol. Struct.*, **267** (1992) 429–34.
16. Chukalin, V. I., Chukanov, N. V., Gurov, S. V., Troitskii, V. N., Filatova, N. E., Rezchikova, T. V. & Domashneva, E. P., Structural special features and infrared spectra of absorption of ultradisperse boron nitride. *Sov. Powder Metall. Met. Ceram.*, **27** (1988) 81–7.
17. Adams, A. C. & Capio, C. D., The chemical deposition of boron–nitrogen films. *J. Electrochem. Soc.*, **127** (1980) 399–405.
18. Cant, N. W. & Little, L. H., Chemisorption sites on porous silica glass and on mixed-oxide catalysts. *Canad. J. Chem.*, **46** (1968) 1373–8.
19. Boehm, H. P. & Knozinger, H., In *Catalysis*, Vol. 4, Springer-Verlag, Berlin, 1983, pp. 39–207.
20. Baraton, M. I., Merle, T., Quintard, P. & Lorenzelli, V., Surface activity of a boron nitride powder: a vibrational study. *Langmuir*, **9** (1993) 1486–91.
21. Busca, G., Lorenzelli, V., Porcile, G., Baraton, M. I., Quintard, P. & Marchand, R., FT-IR study of the surface properties of silicon nitride. *Mater. Chem. Phys.*, **14** (1986) 123–40.
22. Busca, G., Lorenzelli, V., Baraton, M. I., Quintard, P. & Marchand, R., FT-IR characterization of silicon nitride Si_3N_4 and silicon oxynitride Si_2ON_2 surfaces. *J. Mol. Struct.*, **143** (1986) 525–8.
23. Merle, T., Baraton, M. I., Laurent, Y., Quintard, P. & Lorenzelli, V., Reactive sites on AlN surface: a FT-IR starting study. In *Proceedings of the 2nd ECerS Conference*, Vol. 1, 1993, pp. 257–61.
24. Takezawa, N. & Kobayashi, H., On the CH stretching bands of surface alcoholates formed on metal oxides. *J. Catalysis*, **28** (1973) 335–6.
25. Morrow, B. A., Infrared studies of reactions on oxide surfaces. *J. Chem. Soc., Faraday Trans. 1*, **70** (1974) 1527–45.
26. Greenler, R. G., Infrared study of the adsorption of methanol and ethanol on aluminium oxide. *J. Chem. Phys.*, **37** (1962) 2094–100.